# Inhibition of TRPC6 degradation suppresses ischemic brain damage in rats

Wanlu Du, Junbo Huang, Hailan Yao, Kechun Zhou, Bo Duan, and Yizheng Wang

Laboratory of Neural Signal Transduction, Institute of Neuroscience, Shanghai Institutes for Biological Sciences, State Key Laboratory of Neuroscience, The Graduate School, Chinese Academy of Sciences, Shanghai, China.

**Brain injury after focal cerebral ischemia, the most common cause of stroke, develops from a series of pathological processes, including excitotoxicity, inflammation, and apoptosis. While NMDA receptors have been implicated in excitotoxicity, attempts to prevent ischemic brain damage by blocking NMDA receptors have been disappointing. Disruption of neuroprotective pathways may be another avenue responsible for ischemic damage, and thus preservation of neuronal survival may be important for prevention of ischemic brain injury. Here, we report that suppression of proteolytic degradation of transient receptor potential canonical 6 (TRPC6) prevented ischemic neuronal cell death in a rat model of stroke. The TRPC6 protein level in neurons was greatly reduced in ischemia via NMDA receptor–dependent calpain proteolysis of the N-terminal domain of TRPC6 at $Lys^{16}$. This downregulation was specific for TRPC6 and preceded neuronal death. In a rat model of ischemia, activating TRPC6 prevented neuronal death, while blocking TRPC6 increased sensitivity to ischemia. A fusion peptide derived from the calpain cleavage site in TRPC6 inhibited degradation of TRPC6, reduced infarct size, and improved behavioral performance measures via the cAMP response element–binding protein (CREB) signaling pathway. Thus, TRPC6 proteolysis contributed to ischemic neuronal cell death, and suppression of its degradation preserved neuronal survival and prevented ischemic brain damage.**

## Introduction

Stroke is a major cause of death and long-term disability worldwide. Acute ischemic stroke, the most common form, can produce an infarct core, in which the cell death is rapid and irreversible, and a peri-infarct area, in which the cell damage is delayed and rescuable (1, 2). Although several mechanisms, including excitotoxicity, ionic imbalance, oxidative and nitrosative stresses, and apoptosis (1–4), have been implicated in ischemic neuronal death, the $Ca^{2+}$ overload is still the central focus. The NMDA receptor, the important excitatory neurotransmitter receptor in the brain, has been reported as the key player for the $Ca^{2+}$ overload in response to ischemia. However, blocking NMDA receptors to protect ischemic neuronal damage in human clinical trials leads to severe side effects (5–7). Although many factors may have contributed to the unsuccessful trials, it is possible that disruption of neuroprotective pathways could be responsible for the ischemic cell damage. We thus asked whether preserving neuronal survival is critical for brain protection against stroke.

The transient receptor potential canonical (TRPC) is a subfamily of nonselective cation channels permeable to $Ca^{2+}$, which are present in many cell types, including neurons (8–11). The TRPC subfamily with 7 subunits can be divided into 4 subgroups based on their sequence similarity: TRPC1, TRPC2, TRPC3/6/7, and TRPC4/5. Functional TRPC channels are formed by homo- or heterotetramers of these subunits (12, 13). The TRPCs have different roles, including growth cone guidance (14), neurite outgrowth (15), muscle cell proliferation (16), fear memory (17), and neuronal survival (18). These channels can be activated by a phospholipase C–dependent mechanism through activation of both G protein–coupled receptors (GPCR) and receptor tyrosine kinases (13, 19, 20), which have been implicated in neuroprotection in ischemia (21, 22). Therefore, we asked whether TRPC channels play a neuroprotective role against cerebral ischemia.

In this study, we report that the TRPC6 protein in neurons in ischemia was specifically downregulated by the NMDA receptor–dependent calpain proteolysis. Blocking its degradation protected neurons and brains against cerebral ischemia. These results suggest that TRPC6 channels play a critical role in promoting neuronal survival against focal cerebral ischemia and that calpain-mediated downregulation of TRPC6 contributes to ischemic brain injury.

## Results

*The TRPC6 protein in the neurons after ischemia was specifically downregulated*. We first examined the protein levels of TRPCs in a rat model of stroke in which the focal cerebral ischemia was induced by middle cerebral artery occlusion (MCAO) (23) (Supplemental Figure 1; supplemental material available online with this article; doi:10.1172/JCI43165DS1) for 2 hours, which was followed by various periods of reperfusion. Among the examined members of the TRPC subfamily detected with the specific antibodies (Supplemental Figure 2), the protein levels of TRPC6 in the peri-infarct area (ipsilateral cortex) after reperfusion were gradually decreased (Figure 1A) compared with those in the corresponding contralateral cortex. In contrast, the protein levels of TRPC1, -3, -4, and -5, and GluR1 were unaltered (Figure 1B and Supplemental Figure 3A). The quantitative RT-PCR (qRT-PCR) analysis revealed that TRPC6 mRNA levels were unchanged in ischemia (Figure 1C). Additionally, TRPC6 immunoreactivity in neurons in the ipsilateral cortex was markedly reduced 24 hours after reperfusion (Figure 1D). In contrast, TRPC6 immunoreactivity in glial cells was unaltered (Supplemental Figure 3B). In the infarct core region, the protein levels of TRPC4, -5, and -6 were markedly reduced (Supplemental Figure 4). These results indicate that TRPC6 in neurons in the peri-infarct area was specifically downregulated.

**Authorship note:** Wanlu Du, Junbo Huang, and Hailan Yao contributed equally to this work.

**Conflict of interest:** The authors have declared that no conflict of interest exists.

**Citation for this article:** *J Clin Invest.* 2010;120(10):3480–3492. doi:10.1172/JCI43165.

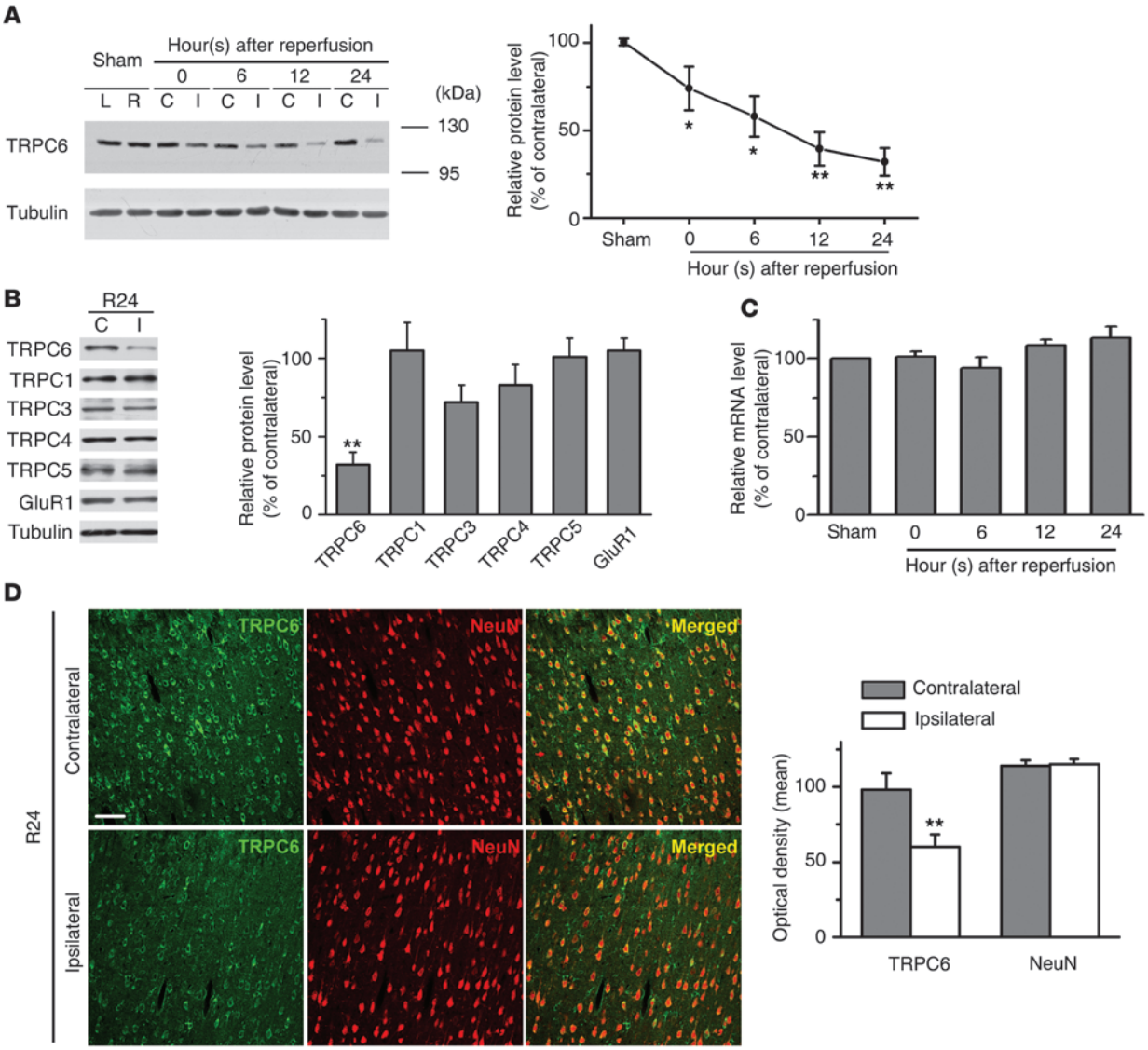


**Figure 1**

TRPC6 in the neurons was downregulated in ischemia. (**A**) Immunoblots of the extracts from the contralateral (C) or ipsilateral (I) cortex (sham; left [L] or right [R] hemisphere) using the indicated antibodies. Tubulin served as a loading control. Right panel: quantification of the normalized TRPC6 protein levels ($n$ = 5–8 rats per time point). *$P$ < 0.05; **$P$ < 0.01 versus sham. (**B**) Immunoblots for TRPCs and GluR1 after 24 hours reperfusion (R24). Right panel: quantification of the protein levels ($n$ = 5 rats). **$P$ < 0.01 versus contralateral. (**C**) TRPC6 mRNA levels determined by qRT-PCR ($n$ = 3–5 rats per time point). (**D**) Representative images of the indicated cortex after 24 hours reperfusion (R24) double-stained with the indicated antibodies. Scale bar: 50 μm. Quantification of the optical density for both TRPC6 and NeuN immunoreactivity is shown on the right panel ($n$ = 5 rats). **$P$ < 0.01 versus the density in contralateral cortex. Data are presented as mean ± SEM. Unless stated, TRPC6 antibody from Millipore was used for Figures 1, 2, and 6 and antibody from Alomone Labs was used for Figures 3, 4, 5, and 7.

*Downregulation of TRPC6 preceded ischemic neuronal cell death*. We then determined whether downregulation of TRPC6 was a concomitant consequence of ischemic neuronal death. In the peri-infarct area, although TRPC6 immunoreactivity was markedly reduced in neurons of ischemic rats 24 hours after reperfusion, cell death (TUNEL-positive cells) became prominent until 48 hours after reperfusion (Figure 2A). Further analysis revealed a negative correlation between the levels of TRPC6 proteins and the numbers of TUNEL-positive cells during reperfusion. As shown in Figure 2B, the levels of TRPC6 proteins were greatly decreased at the beginning of reperfusion and the reduction in TRPC6 protein levels remained prominent 12, 24, and 48 hours after reperfusion. In contrast, the numbers of TUNEL-positive cells were gradually or markedly increased 24 hours or 48 hours, respectively, after reperfusion. Therefore, downregulation of TRPC6 took place prior to and during the occurrence of ischemic neuronal cell death. These results suggest that reduction in TRPC6 levels may play a role in ischemic brain injury.

*Downregulation of TRPC6 in modeled ischemia was responsible for neuronal cell death*. To study whether TRPC6 is functionally downregulated under ischemic conditions, we examined TRPC6 protein levels in the neurons deprived of oxygen and glucose (OGD),

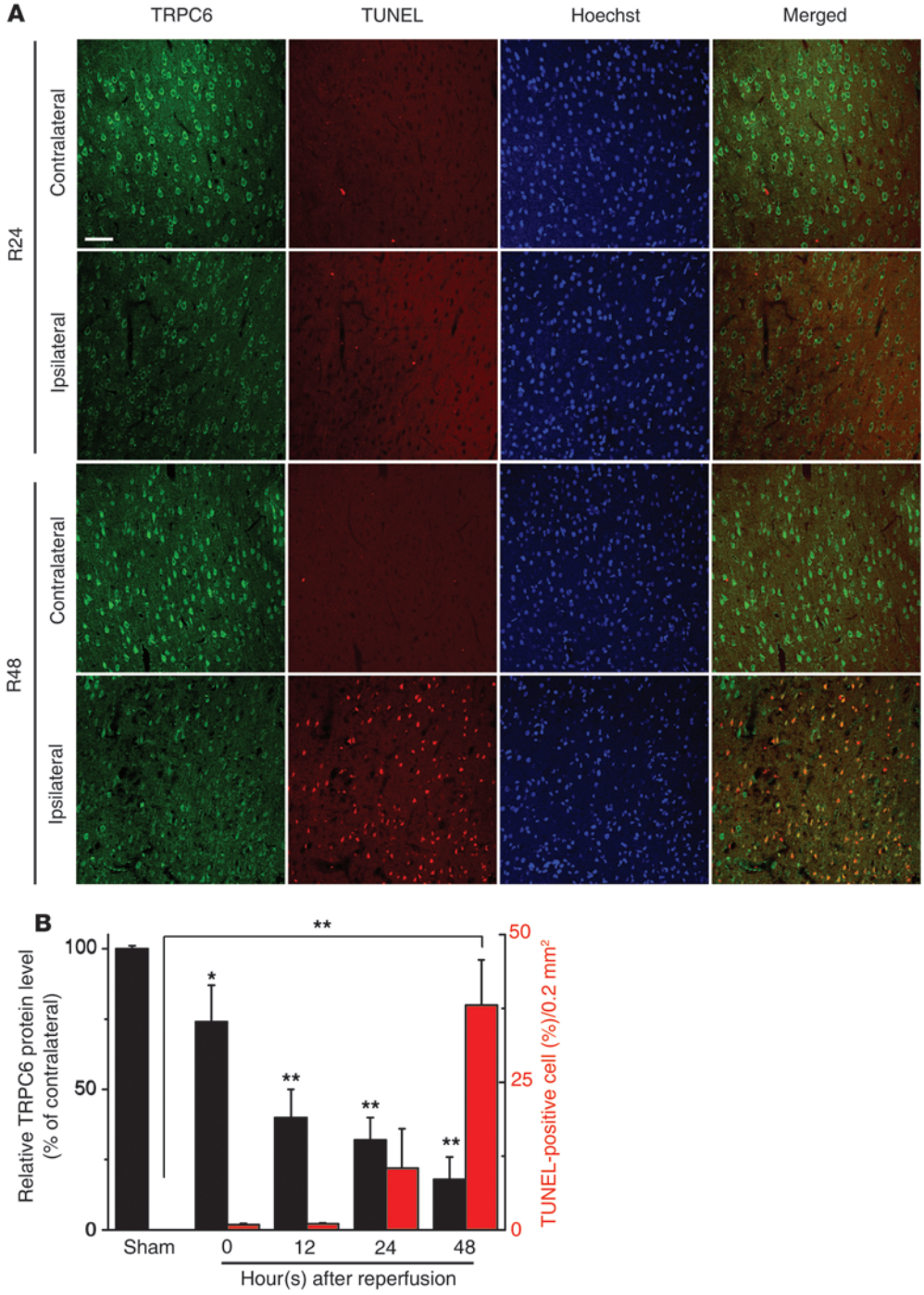


**Figure 2**
Downregulation of TRPC6 was prior to and during ischemic neuronal death. (**A**) Representative images of the indicated cortex after 24 hours (R24) or 48 hours (R48) reperfusion double stained with TRPC6 antibody (Millipore) and TUNEL labeling. Hoechst stain was used to label the nucleus. Scale bar: 50 μm. (**B**) Quantification of the levels of TRPC6 and the numbers of TUNEL-positive cells in the ipsilateral cortex at the indicated times or sham surgery (sham) ($n$ = 3 rats for each condition). $^{*}P < 0.05$; $^{**}P < 0.01$ versus sham. Data are presented as mean ± SEM.

a common ischemia model in vitro (24). The protein levels of TRPC6, but not TRPC3, were greatly reduced following OGD (Figure 3A). However, the mRNA levels for TRPC1, -3, and -6 were unchanged after OGD (Supplemental Figure 3C). We then examined TRPC6 channel activity by the whole-cell patch recording on the cortical neurons after OGD. In neurons, a sustained inward current was induced by 1-oleoyl-2-acetyl-*sn*-glycerol (OAG), a membrane-permeable diacylglycerol (DAG) analog known to activate TRPC3/6 channels (25). This OAG-induced inward current ($I_{OAG}$) was blocked by N-methyl-D-glucamine (NMDG, to replace $Ca^{2+}$ and $Na^{+}$) and SKF96365, an agent known to inhibit TRPC activity (26, 27), or when TRPC6 expression was specifically downregulated by the RNAi construct against TRPC6 (RNAi_C6; Figure 3B). Furthermore, OAG induced an elevation in intracellular $Ca^{2+}$ concentration ($[Ca^{2+}]_i$) as determined by fluorescence ratio imaging of $Ca^{2+}$ in cultured cortical neurons. This elevation was suppressed by SKF96365 or when the neurons were incubated in the $Ca^{2+}$-free medium or transfected with a dominant-negative form of TRPC6 (DN-TRPC6), known to suppress TRPC6 channel activity (28) (Supplemental Figure 5).

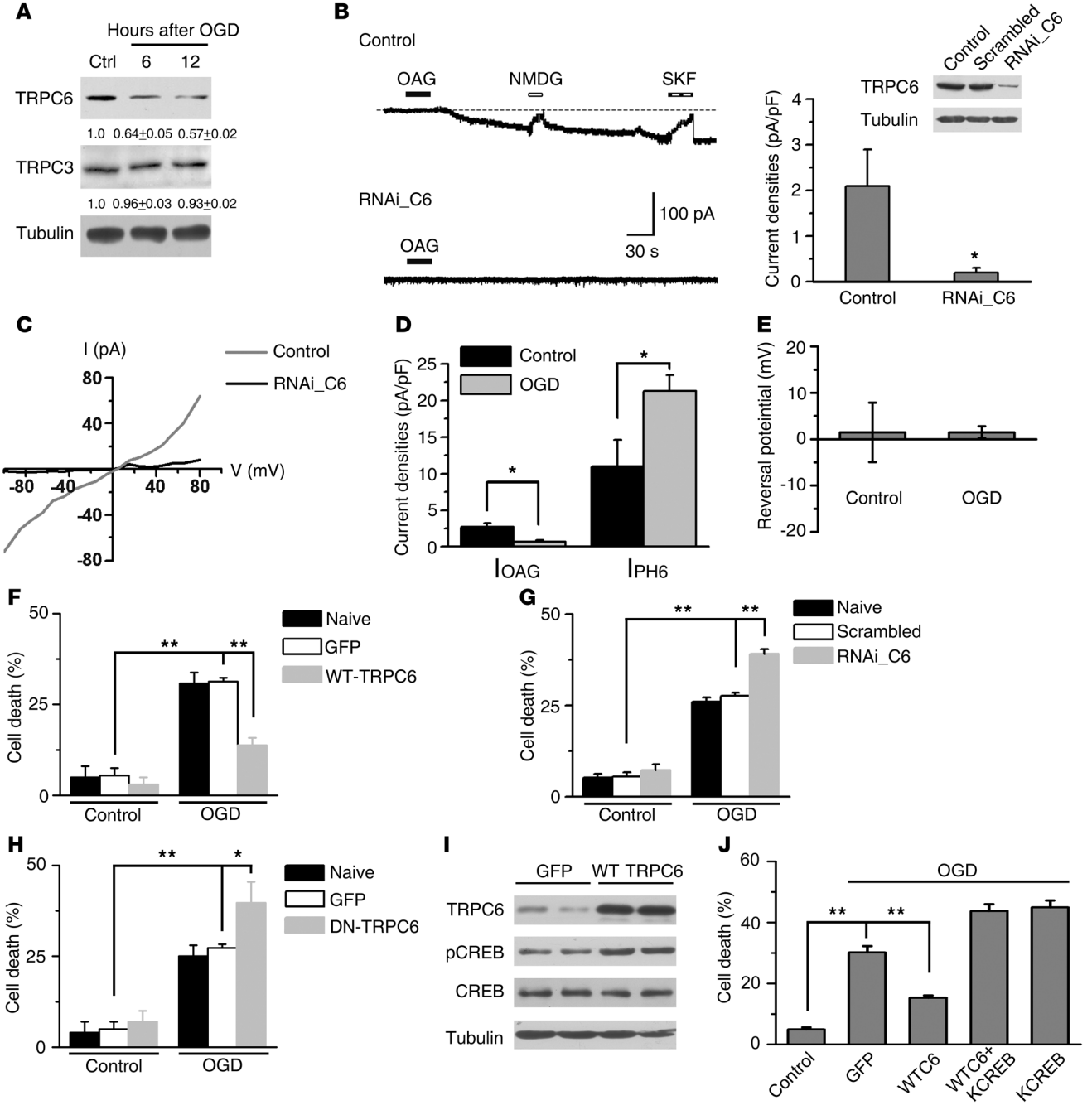


**Figure 3**

TRPC6 was downregulated in modeled ischemia. (**A**) Immunoblots of the extracts from cultured cortical neurons after OGD with indicated antibodies. The numbers below the blots are the normalized protein levels ($n = 3$). (**B**) Whole-cell recording for cultured cortical neurons (upper trace, control) or neurons transfected with RNAi_C6 (lower trace, RNAi_C6). Right panel: quantification of the current density. Islet: representative blots for TRPC6. OAG (100 μM); SKF, SKF96365 (10 μM). NMDG in $Ca^{2+}$-free solution ($n = 10$ cells for control group; $n = 8$ cells for RNAi_C6 group). $^*P < 0.05$ versus control. (**C**) I/V relationship of the OAG-induced currents from untransfected (control) or RNAi_C6-transfected neurons (RNAi_C6). Quantification of the indicated current densities (**D**) or the reversal potential of $I_{OAG}$ (**E**) from control or OGD-treated neurons. $^*P < 0.05$ versus control. (**F**–**H**) Quantification of cell death for the neurons transfected with the constructs, subjected to OGD followed by 24 hours incubation ($n = 3$). $^*P < 0.05$; $^{**}P < 0.01$ versus GFP or scrambled. (**I**) Immunoblots of the extracts from the neurons transfected with GFP or WT TRPC6 using the indicated antibodies. (**J**) Cortical neurons transfected with the constructs subjected to OGD and cell death assessed by PI staining. KCREB, dominant-negative form of CREB ($n = 3$). $^{**}P < 0.01$ versus GFP. Data are presented as mean ± SEM.

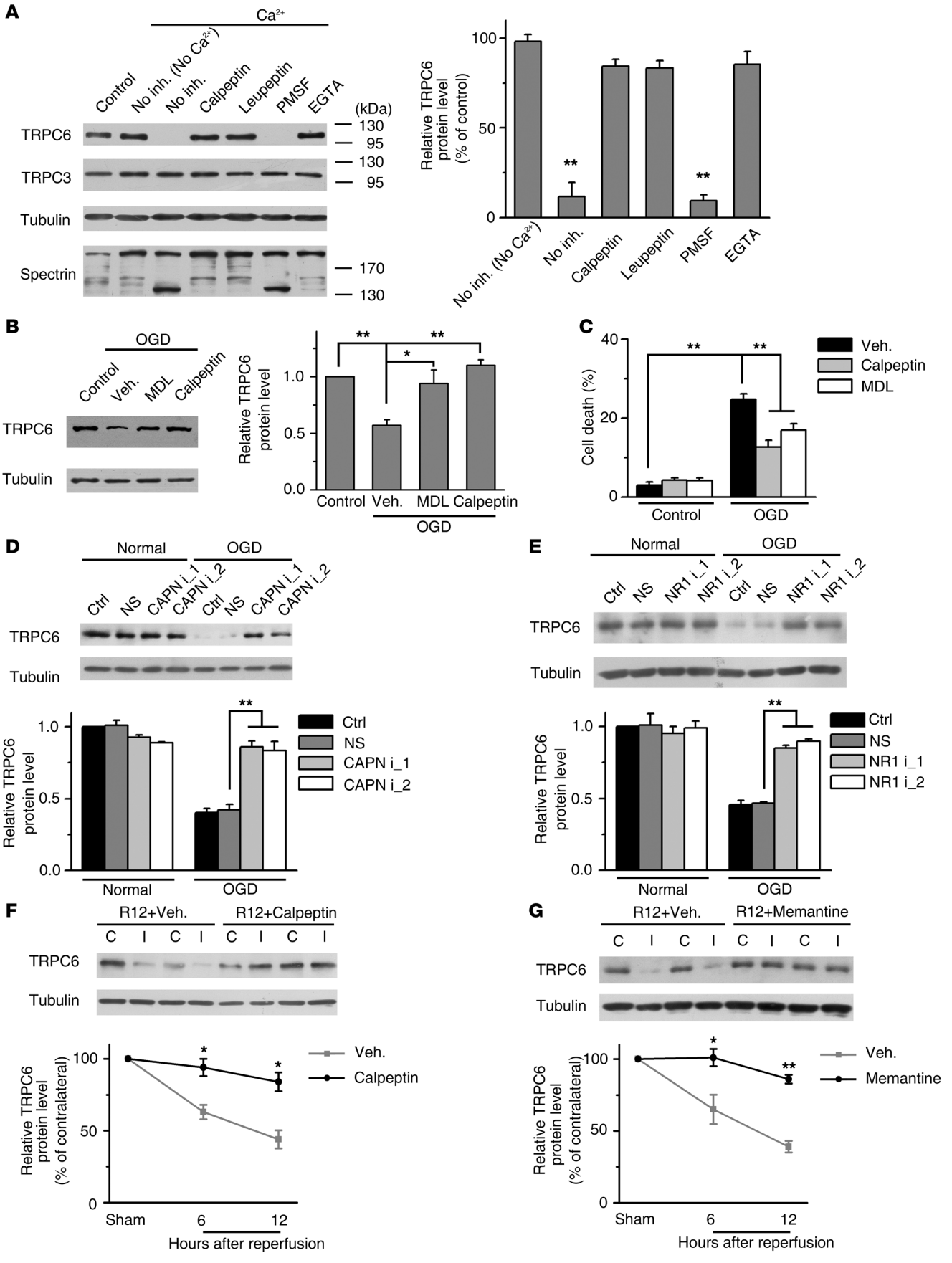
A
Ca2+
Control
No inh. (No Ca2+)
No inh.
Calpeptin
Leupeptin
PMSF
EGTA
(kDa)
TRPC6
TRPC3
Tubulin
Spectrin
130
95
130
95
170
130
Relative TRPC6 protein level (% of control)
100
50
0
**
**
No inh. (No Ca2+)
No inh.
Calpeptin
Leupeptin
PMSF
EGTA
B
OGD
Control
Veh.
MDL
Calpeptin
TRPC6
Tubulin
Relative TRPC6 protein level
1.0
0.5
0.0
**
**
*
Control
Veh.
MDL
Calpeptin
OGD
C
Cell death (%)
40
20
0
**
**
Veh.
Calpeptin
MDL
Control
OGD
D
Normal
OGD
Ctrl
NS
CAPN i_1
CAPN i_2
Ctrl
NS
CAPN i_1
CAPN i_2
TRPC6
Tubulin
Relative TRPC6 protein level
1.0
0.5
0.0
**
Ctrl
NS
CAPN i_1
CAPN i_2
Normal
OGD
E
Normal
OGD
Ctrl
NS
NR1 i_1
NR1 i_2
Ctrl
NS
NR1 i_1
NR1 i_2
TRPC6
Tubulin
Relative TRPC6 protein level
1.0
0.5
0.0
**
Ctrl
NS
NR1 i_1
NR1 i_2
Normal
OGD
F
R12+Veh.
R12+Calpeptin
C
I
C
I
C
I
C
I
TRPC6
Tubulin
Relative TRPC6 protein level (% of contralateral)
100
50
0
*
*
Veh.
Calpeptin
Sham
6
12
Hours after reperfusion
G
R12+Veh.
R12+Memantine
C
I
C
I
C
I
C
I
TRPC6
Tubulin
Relative TRPC6 protein level (% of contralateral)
100
50
0
*
**
Veh.
Memantine
Sham
6
12
Hours after reperfusion

**Figure 4**
NMDAR-mediated calpain proteolysis of TRPC6 in modeled ischemia. (**A**) TRPC6 was proteolyzed by calpain. Immunoblots of the rat brain lysates incubated with $Ca^{2+}$ in the presence or absence (No inh.) of the indicated agents using the indicated antibodies. Calpeptin, 20 μM; leupeptin, 100 μM; PMSF, 100 μM; EGTA, 5 mM. Right panel: quantification of TRPC6 levels ($n$ = 3). $^{**}P < 0.01$ versus control. (**B**) Immunoblots for TRPC6 in cortical neurons 24 hours after OGD in the presence of vehicle (Veh.), calpeptin (20 μM), or MDL28170 (MDL, 60 μM). Right panel: quantification of TRPC6 levels ($n$ = 3). $^{*}P < 0.05$; $^{**}P < 0.01$ versus vehicle (TRPC6 antibody: Sigma-Aldrich). (**C**) Quantification of OGD-induced cell death (at 24 hours) in the presence of vehicle, calpeptin, or MDL28170 ($n$ = 3). $^{**}P < 0.01$ versus vehicle. (**D**) 2 calpain siRNA prevented OGD-induced TRPC6 degradation. Lower panel: quantification of TRPC6 levels ($n$ = 3). $^{**}P < 0.01$ versus nonsense siRNA (NS). (**E**) 2 NR1 siRNA inhibited OGD-induced TRPC6 degradation. Right panel: quantification of TRPC6 levels ($n$ = 3) $^{**}P < 0.01$ versus NS. Calpeptin (**F**) or memantine (**G**) suppressed the ischemia-induced TRPC6 degradation as analyzed by immunoblots. Quantifications of TRPC6 levels are shown on the lower panel. R12, 12 hours after reperfusion ($n$ = 3). $^{**}P < 0.01$ versus vehicle. Data are presented as mean ± SEM.

The double-rectifying property obtained from I/V curve analysis (Figure 3C) showed the characteristics of the TRPC currents. Together, these results suggest that the OAG-induced current in the neurons was predominantly mediated by TRPC6. In the neurons upon OGD, the $I_{OAG}$ was markedly suppressed, whereas, as reported, the $I_{pH}6.0$ (the current of acid-sensing ion channels) was increased (29) (Figure 3D). These results suggest that TRPC6 channel activity was specifically inhibited. Moreover, the reversal potential in control and OGD was not different (Figure 3E). Thus, downregulation of TRPC6 in the neurons upon OGD suppressed $I_{OAG}$.

We next tested to determine whether increasing TRPC6 protein levels could prevent neuronal death induced by OGD. The neurons were transfected with GFP-tagged TRPC6 (WT-TRPC6), DN-TRPC6, or the RNAi_C6. The TRPC6 overexpression in the neurons was verified by immunoblotting 11 days after electroporation (Supplemental Figure 6A). The OGD-induced cell death was greatly suppressed in the cultures transfected with TRPC6 (Figure 3F). It has been reported that activation of cAMP response element–binding protein (CREB) is important for neuroprotection against ischemia (30, 31) and that $Ca^{2+}$ influx through TRPC6 contributes to CREB activation (18). Indeed, we found that overexpressing TRPC6 enhanced the levels of phosphorylated CREB at Ser133 (p-CREB), an activated form of CREB (Figure 3I). Moreover, TRPC6 prevented ischemic neuronal death via a CREB-dependent mechanism, since overexpressing KCREB, a dominant negative form of CREB, abolished the neuroprotective effect of TRPC6 (Figure 3J). Conversely, expressing RNAi_C6 or DN-TRPC6 increased sensitivity to ischemic insults (Figure 3, G and H). Consistently, OAG or SKF96365 suppressed or enhanced cell death induced by OGD and ischemia, respectively (Supplemental Figure 6, B–D). These results suggest that TRPC6 in modeled ischemia was functionally downregulated and that increase in its protein level or activity prevented neuronal death.

*NMDARs mediated calpain proteolysis of TRPC6 in modeled ischemia.* The rapid reduction in TRPC6 protein levels after ischemia (Figure 1A) suggests that it may be degraded by a protease. Additional studies were carried out to determine the possible protease that mediated TRPC6 degradation. In cortical extracts, the TRPC6, but not TRPC3, protein was rapidly degraded in the presence of $Ca^{2+}$ and the $Ca^{2+}$-induced TRPC6 degradation was time and dose dependent (Supplemental Figure 7, A and B), blocked by EGTA and associated with calpain activation as indicated by spectrin degradation (32) (Figure 4A and Supplemental Figure 7C). Furthermore, PMSF, the serine protease inhibitor, cpm-VAD-CHO, the caspase inhibitor, and lactacystin, the proteasome inhibitor, all did not affect the $Ca^{2+}$-induced TRPC6 degradation. In contrast, the calpain inhibitors, including calpeptin, leupeptin, and MDL28170, all prevented TRPC6 degradation (Figure 4A and Supplemental Figure 7C). Thus, TRPC6 was likely proteolyzed by calpain.

We then determined whether TRPC6 downregulation was indeed mediated by calpain proteolysis in modeled ischemia. Both calpeptin and MDL28170 blocked OGD-induced TRPC6 degradation and cell death (Figure 4, B and C). Moreover, knocking down calpain by specific siRNAs (Supplemental Figure 7D) blocked the TRPC6 degradation (Figure 4D). It has been reported that calpain can be activated by $Ca^{2+}$ influx through N-methyl-D-aspartate receptors (NMDARs) during ischemia (33–35). Indeed, we found that calpain was activated in ischemia/reperfusion (Supplemental Figure 7E). MK801, a known NMDAR blocker, prevented TRPC6 degradation induced by OGD (Supplemental Figure 7F), and knocking down NR1, an indispensable subunit of NMDARs, by 2 NR1-specific siRNAs (Supplemental Figure 7G), blocked the OGD-induced TRPC6 degradation (Figure 4E). Furthermore, in the MCAO model, intracerebroventricular preinjection of calpeptin or memantine (the NMDAR blocker) markedly inhibited TRPC6 degradation (Figure 4, F and G). These results suggest that in ischemia, calpain proteolysis of TRPC6 was mediated by NMDARs.

*The TRPC6 protein was proteolyzed by calpain at $K^{16}$ and $A^{17}$.* To confirm that TRPC6 was directly proteolyzed by calpain, we transfected HEK293 cells with the N-terminal *flag*-, second extracellular loop *HA*-, and C-terminal *myc*-tagged TRPC6 construct (Figure 5A). The cell lysates were incubated with different concentrations of purified μ-calpain, known as the main isoform of calpain found in neurons (36), and immunoblotted with the anti-tag antibodies. As detected with anti-*HA* antibody, μ-calpain dose dependently reduced the levels of TRPC6 with a concomitant appearance of 2 bands with smaller molecular weights (Figure 5A). The reduction in TRPC6 levels detected by anti-*flag* antibody was more sensitive to calpain digestion than that detected by anti-*myc* antibody, and a fragment below the full-length TRPC6 was detected by anti-*myc*, but not anti-*flag*, antibody (Figure 5A). These results indicate that the N terminus of TRPC6 was more sensitive to calpain proteolysis and that calpain sequentially cleaved the TRPC6 protein. We thus made a construct in which the N terminus of TRPC6 (from $M^1$ to $D^{203}$) was fused to the NUS-tag (NUS_$C6_{1–203}$). After calpain digestion of the purified NUS_$C6_{1–203}$, a 22-kDa fragment was found (Figure 5B). The N terminus of this fragment was sequenced to be AAPGA with Edman degradation, demonstrating that the calpain cleavage site in TRPC6 was between $K^{16}$ and $A^{17}$ (Figure 5B). Two–amino acid deletion surrounding the cleavage site (TRPC6$\Delta_{16-17}$) inhibited the calpain proteolysis of TRPC6 (Supplemental Figure 8A), supporting that the cleavage between $K^{16}$ and $A^{17}$ in TRPC6 plays a critical role in triggering loss of the protein. To prevent the cleavage of TRPC6, a TAT-C6 peptide was designed to generate a cell-permeable peptide (37) that contained a sequence spanning the calpain cleavage site in TRPC6 (Figure 5B). The TAT-C6 peptide dose dependently inhibited $Ca^{2+}$-induced TRPC6, but not spectrin, degradation in the cortical extracts (Figure 5C).

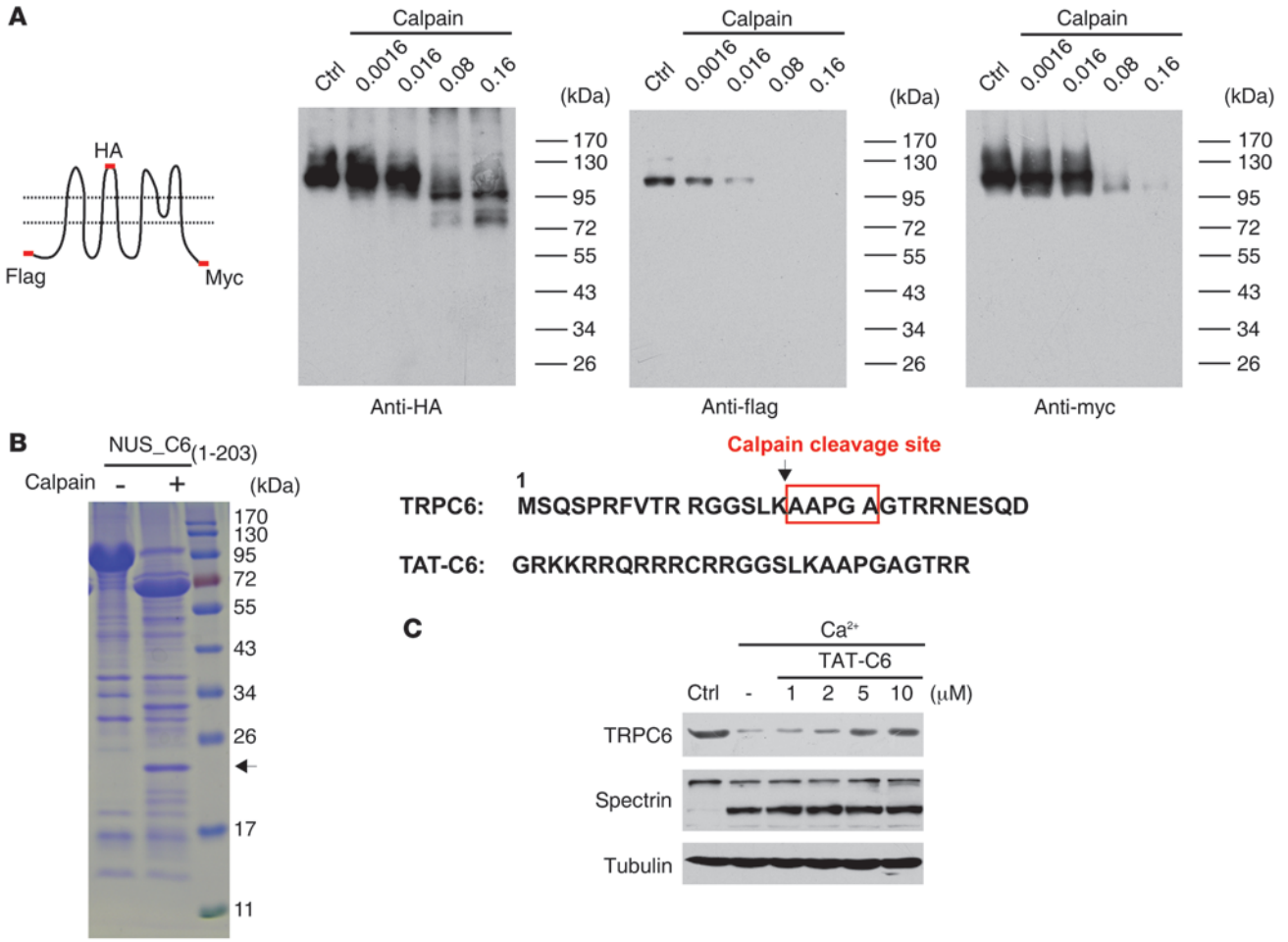


**Figure 5**

TRPC6 was cleaved by calpain at Lys[16]. (**A**) Immunoblots of the lysates from HEK293 cells transfected with the TRPC6 tagged with N-*flag*-second loop-*HA*-C-*myc* (the schematic) and incubated with μ-calpain at the indicated concentrations using the indicated antibodies. (**B**) Purified NUS_C6$_{1\text{-}203}$ was digested with calpain and stained with Coomassie blue. Arrow indicates a 22-kDa fragment, whose N-terminal sequence is shown on the right. Lower sequence shows TAT-C6. (**C**) Immunoblots of the rat brain lysates incubated with 1 mM $Ca^{2+}$ for 30 minutes in the presence of the indicated concentrations of TAT-C6 peptide using the indicated antibodies.

*The TAT-C6 was neuroprotective in modeled ischemia*. We further detected whether the TAT-C6 protects neurons in modeled ischemia. Neurons were incubated with a control peptide or TAT-C6 and then subjected to OGD. As shown in Figure 6, the number of TUNEL-positive cells in OGD was greatly increased compared with that in normoxia, and the control peptide did not affect cell survival. In contrast, the number of TUNEL-positive cells in OGD in the presence of TAT-C6 was markedly reduced compared with that in OGD in the presence of the control peptide (TAT-ctrl) (Figure 6, A and B). To detect whether the N-terminal fragment of TRPC6 produced by calpain cleavage may have contributed to the neurotoxicity or protection, we synthesized the N-terminal fragment fused with the TAT peptide (TAT-C6-N15) and examined its effect on neuronal survival. As shown in Supplemental Figure 9, the peptide did not affect neuronal survival. We then detected CREB activity in neuron cultures before and after OGD. The levels of p-CREB in OGD groups were greatly reduced compared with those in control groups. Preincubation with TAT-C6 peptide markedly reversed the reduction in p-CREB levels (Figure 6C). These results indicate that the TAT-C6 peptide indeed maintained CREB activity and protected neurons from ischemic insults.

*Inhibiting calpain-mediated TRPC6 degradation prevented ischemic brain damage*. Our in vivo and in vitro results suggest that ischemic neuronal cell death was associated with the reduction in TRPC6 protein levels. To directly show that inhibition of calpain-mediated TRPC6 degradation in neurons indeed prevented ischemic brain damage, we intracerebroventricularly preinjected the TAT-C6 peptide and assessed the infarct volume in a double-blinded manner. As shown in Figure 7, A and B, TRPC6 degradation or infarct volume in ischemia was greatly prevented or reduced, respectively, in TAT-C6 groups. Moreover, the TAT-C6 peptide specifically inhibited TRPC6 degradation, but not spectrin cleavage, after ischemia. In the rotarod test, the rats preinjected with the TAT-C6 showed a marked improvement in behavior performance compared with those preinjected with TAT-ctrl (Figure 7C). This improvement in behavior performance was found 35 days after ischemia (Figure 7C). Furthermore, the mortality of TAT-C6

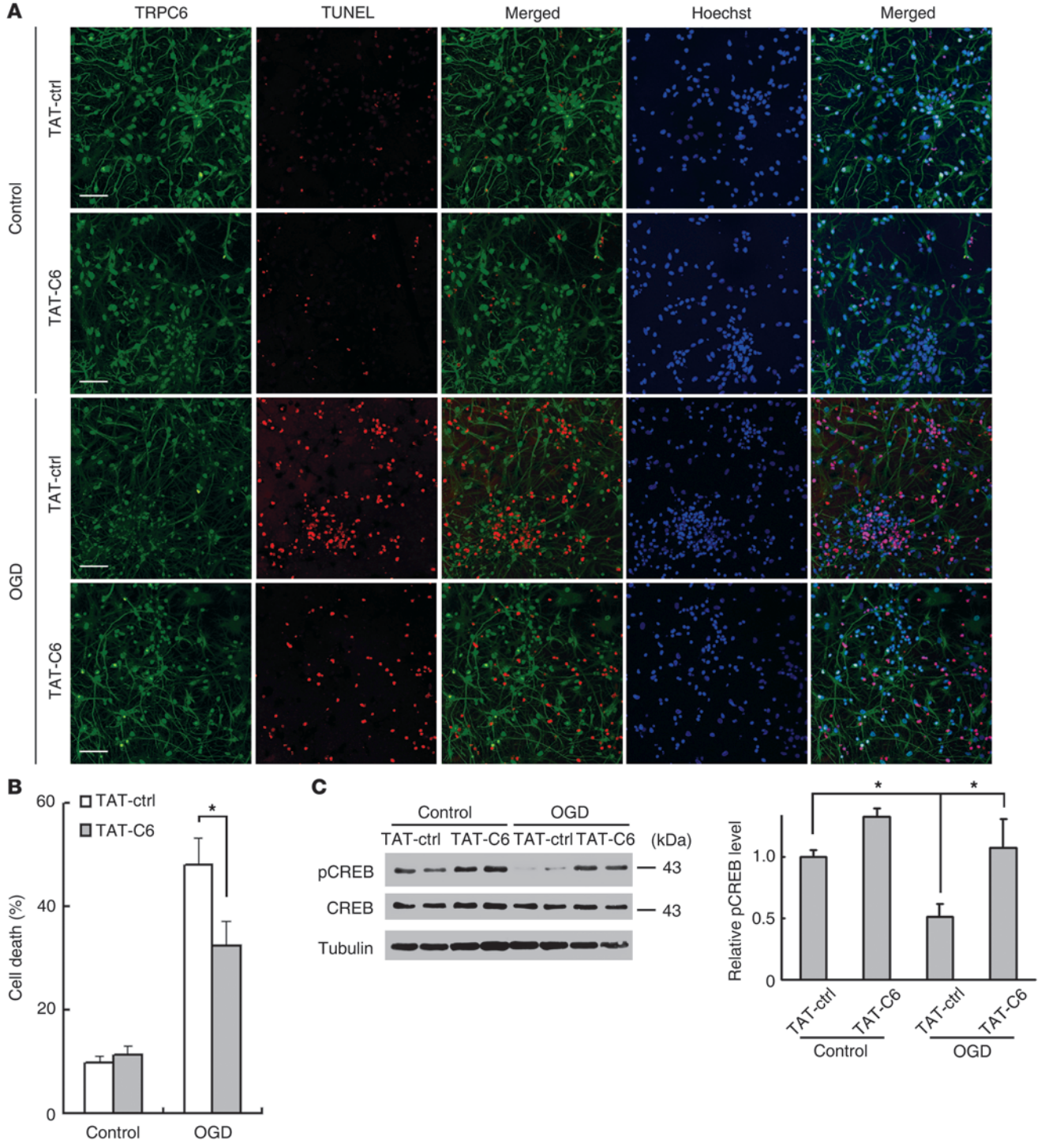


**Figure 6**

TAT-C6 inhibited neuronal cell death induced by OGD. (**A**) Representative images of cortical neurons incubated with 5 μM TAT-ctrl or TAT-C6 2 hours before OGD and double stained with TRPC6 antibody and TUNEL labeling 24 hours after OGD. Hoechst stain was used to label the nucleus. Scale bars: 50 μm. (**B**) Quantification of OGD-induced cell death (at 24 hours) in the presence of TAT-ctrl or TAT-C6. *$P < 0.05$ versus TAT-ctrl. (**C**) Immunoblots for CREB and pCREB of the extracts from OGD-treated cortical neurons receiving TAT-ctrl or TAT-C6. Right panel shows quantification of p-CREB levels ($n$ = 3–6 cultures). *$P < 0.05$ versus control or TAT-ctrl. Data are presented as mean ± SEM.

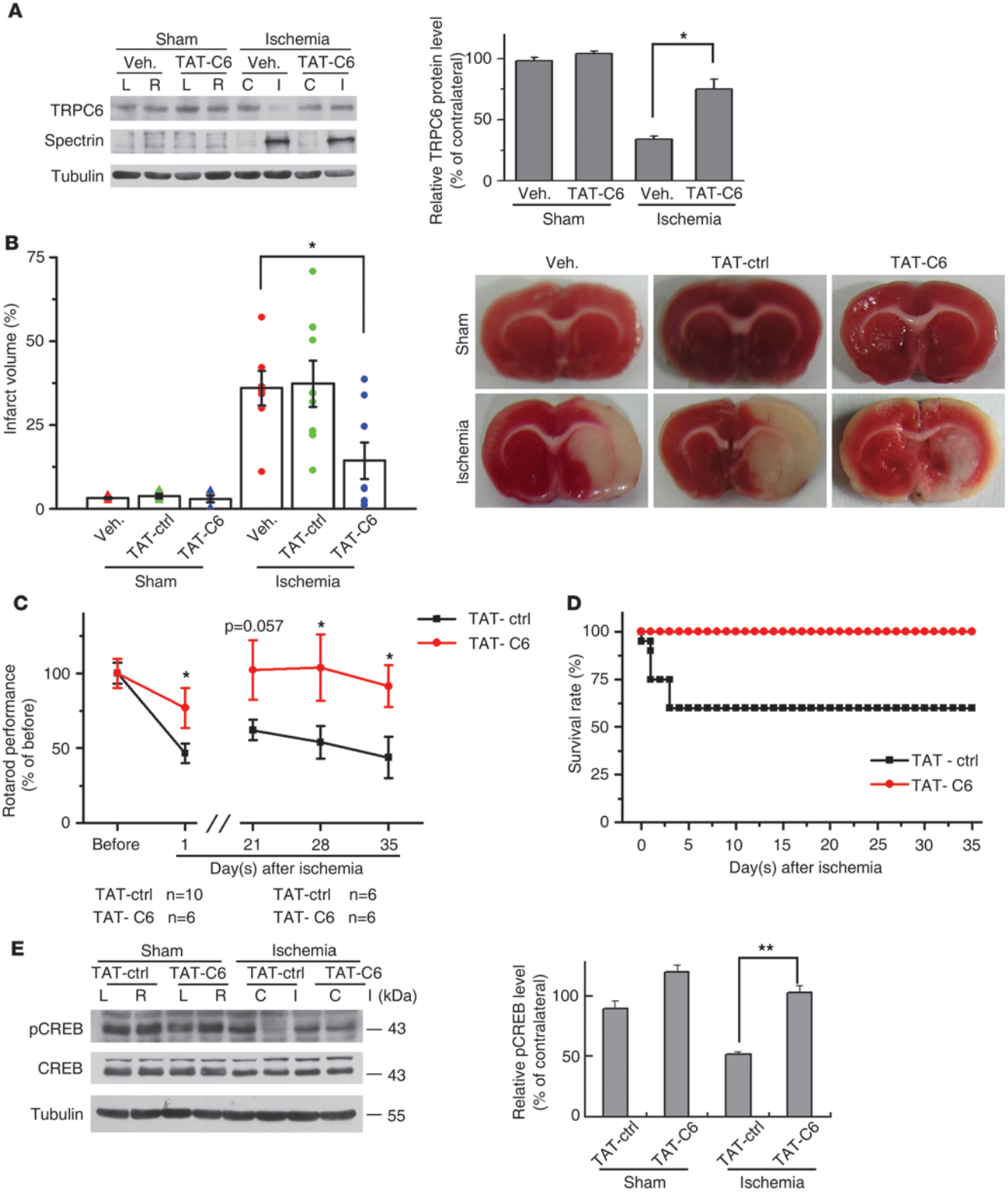
A
Sham
Ischemia
Veh.
TAT-C6
Veh.
TAT-C6
L R L R C I C I
TRPC6
Spectrin
Tubulin
Relative TRPC6 protein level (% of contralateral)
100
50
0
*
Veh. TAT-C6 Veh. TAT-C6
Sham
Ischemia
B
Infarct volume (%)
75
50
25
0
*
Veh.
TAT-ctrl
TAT-C6
Veh.
TAT-ctrl
TAT-C6
Sham
Ischemia
Veh.
TAT-ctrl
TAT-C6
Sham
Ischemia
C
Rotarod performance (% of before)
100
50
0
p=0.057
*
*
*
TAT- ctrl
TAT- C6
Before
1
21
28
35
Day(s) after ischemia
TAT-ctrl n=10
TAT- C6 n=6
TAT-ctrl n=6
TAT- C6 n=6
D
Survival rate (%)
100
75
50
25
0
TAT - ctrl
TAT- C6
0 5 10 15 20 25 30 35
Day(s) after ischemia
E
Sham
Ischemia
TAT-ctrl
TAT-C6
TAT-ctrl
TAT-C6
L R L R C I C I (kDa)
pCREB
CREB
Tubulin
43
43
55
Relative pCREB level (% of contralateral)
100
50
0
**
TAT-ctrl
TAT-C6
TAT-ctrl
TAT-C6
Sham
Ischemia

**Figure 7**
Inhibiting calpain-mediated TRPC6 degradation protected rat brains from ischemic damage. (**A**) Immunoblots for TRPC6 and spectrin in the cortical extracts from ischemic or sham-treated rats receiving vehicle or TAT-C6 peptide (TAT-C6). Right panel: quantification of TRPC6 protein levels ($n$ = 3 rats). *$P$ < 0.05 versus vehicle. (**B**) TTC-stained brain sections indicated the infarct volumes (bar graph) or area (image) in rats receiving vehicle, control TAT-peptide (TAT-ctrl), or TAT-C6 peptide after ischemia ($n$ = 8 rats). *$P$ < 0.05 versus vehicle. (**C**) Rotarod evaluation of the 2 groups of rats, showing behavioral improvement. Upper curve, rats injected with TAT-C6; lower curve, rats injected with TAT-ctrl. *$P$ < 0.05 versus TAT-ctrl (below, number of rats used for statistical analysis). (**D**) Survival rates of rats injected with TAT-C6 or TAT-ctrl ($n$ = 6 for TAT-C6 group; $n$ = 10 for TAT-ctrl group) after cerebral ischemia. (**E**) Immunoblots for CREB and pCREB in the cortical extracts from ischemic or sham-treated rats receiving TAT-ctrl or TAT-C6. Right panel: quantification of pCREB levels ($n$ = 3 rats). **$P$ < 0.01 versus TAT-ctrl. Data are presented as mean ± SEM.

groups was much lower than that of TAT-ctrl groups (Figure 7D). We also determined CREB activity by measurement of p-CREB (Ser-133) levels in the cortical extracts. The p-CREB levels in ischemic groups were markedly reduced compared with those in sham groups. Injection of TAT-C6 peptide substantially reversed the reduction in p-CREB levels (Figure 7E). Moreover, the improvement in behavior performance and reduction in mortality in TAT-C6 groups were associated with the maintenance of the levels of p-CREB. These results are thus consistent with the explanation that TRPC6 promotes activation of CREB to protect neurons against ischemia. Together, these results suggest that preventing calpain-mediated TRPC6 degradation did maintain the integrity of the circuitry to improve their behavior outcome and protect rats from ischemic brain damage.

## Discussion

In cerebral ischemia, both detrimental and protective pathways could affect the pathological processes of brain damage. The unsuccessful results of clinical trials to prevent ischemic brain injury by blocking the detrimental pathways support search for new mechanisms or targets for neuroprotection in stroke. Here we showed that inhibition of calpain proteolysis of TRPC6 protected rats from ischemic brain damage. Several lines of evidence support this conclusion. First, TRPC6 was specifically degraded in transient ischemia and this degradation occurred prior to and during the neuronal cell death (Figures 1 and 2). Second, TRPC6 function was suppressed in modeled ischemia. Maintaining its expression was neuroprotective via the CREB-dependent mechanism (Figures 3 and 7E). Third, NMDARs mediated calpain proteolysis of TRPC6 (Figure 4). Finally, inhibition of calpain proteolysis of TRPC6 by the TAT-C6 peptide protected animals from ischemic brain damage and improved their behavior performance after stroke (Figure 7, B–D). We thus propose that both detrimental and protective signalings greatly influence ischemic brain damage, in which TRPC6 protects neurons against ischemic insults. Therefore, inhibition of TRPC6 degradation to preserve neuronal survival could be a new preventive strategy against ischemic brain damage.

Brain injury affects neuroprotective pathways that maintain ionic homeostasis (38), among which CREB plays a pivotal role in preserving neuronal survival (39, 40). Our results are consistent with a model in which inhibition of the TRPC6/CREB pathway may contribute to ischemic brain damage. It is possible that suppression of CREB as a result of TRPC6 downregulation inhibits the expression of survival factors, including BDNF and Bcl-2 (41), which may affect neuronal survival in ischemia. Neuronal damage in ischemia can cause deficits in motor circuitry, resembling the palsy of embolic stroke patients (42). Blocking TRPC6 degradation maintained phosphorylation of CREB and greatly improved behavior performance (Figure 7C), supporting the idea that the TRPC6/CREB pathway is important for maintaining neuronal circuitry after stroke.

A notable phenomenon is that TRPC6, as a member of the TRPC subfamily, is implicated in ischemic neuronal survival, whereas TRPM7 is implicated in ischemic neuronal death (43, 44). The diversity in activation mechanisms of TRP channels might contribute to the difference. It has been reported that TRPM7 is directly activated by ROS (reactive oxygen/nitrogen species) (43), which induces neuronal damage in pathological conditions (45, 46). In contrast, TRPC6 is activated by both receptor tyrosine kinases and GPCRs, molecules known to be important for neuronal survival (18, 47, 48). It is thus possible that TRPC6 preserves neuronal survival likely via transmitting survival signals in ischemia. Additionally, TRPM7 may act upstream from excitotoxicity in ischemic neuronal damage (43, 44). In contrast, TRPC6 mediates neuroprotective effects, a possible role of TRPC6 in brain development (18). Furthermore, the divalent cation selectivity of TRPC6 and TRPM7 is different (49). Owing to the high divalent cation selectivity, activation of TRPM7-containing channels in ischemia leads to $Ca^{2+}$ overload, ROS production, and subsequent ischemic cell death. In contrast, a modest level of $Ca^{2+}$ influx through TRPC6 channels leads to activation of both ERK and CaMK, which converge on CREB to promote neuronal survival.

It should be pointed out that TRPC6, but not other members of the TRPC subfamily, was degraded in ischemia. Sequence alignments among TRPC3, -6, and -7 revealed that the first 60 amino acids in their N termini are very different although the sequence similarity of these subunits is higher than 60%. The alignment analysis also showed that the cleavage site found here in TRPC6 is unique among these subunits (Supplemental Figure 8B). The sequence difference in the cleavage site may explain why only TRPC6 was proteolytically degraded by calpain. We did not find upregulation of TRPC3 in ischemia (data not shown), although TRPC3 mRNA expression is increased in TRPC6 knockout mice (50). Moreover, TRPC6 and -3 are not freely functionally interchangeable (50–52). In our study, focal cerebral ischemia was transient; it is thus possible that no compensatory effect of other members of TRPCs could take place in such a short period of time.

Our inability to detect in vivo the TRPC6 cleavage product that was found in vitro in cultured cells (Figure 5A) suggested that this protein after the initial cleavage is not stable in vivo (Figure 1A). The mechanism by which its complete degradation is controlled is not clear at the present time. Since prolonged incubation with calpain resulted in TRPC6 complete degradation (Figure 5A), it is possible that calpain mediates its complete degradation, a process similar to calpain-mediated proteolysis of p53 (53). Additionally, the N-terminal cleavage of TRPC6 is likely a prerequisite for its complete degradation, probably via the ubiquitin proteasome system, resembling the calpain-mediated cleavage of talin (54), which is cleaved by calpain and further degraded by the ubiquitin proteasome system. Consistently, 2–amino acid deletion surrounding the cleavage site in TRPC6 inhibited calpain proteolysis of TRPC6 (Supplemental Figure 8A). Calpain cleavage could produce frag-

ments with a function (55). Since TAT-C6-N15 did not affect neuronal survival, it is unlikely that the N-terminal cleavage fragment of TRPC6 was neurotoxic or protective.

In conclusion, our results suggest that activation of NMDA receptors and calpain leads to TRPC6 degradation and neuronal damage in ischemia. Thus, activation of the detrimental pathways, such as NMDAR/calpain, may disrupt the protective pathways, such as TRPC6/CREB, resulting in neuronal damage and subsequent ischemic brain injury. In this context, preventing degradation of TRPC6 by the TAT-C6 peptide could be a new strategy for alleviation of ischemic brain damage.

## Methods

*Animal experiments*. The experimental protocols were approved by the Institutional Animal Care and Use Committee of the Institute of Neuroscience, Shanghai, China. Focal cerebral ischemia was induced by MCAO (the suture method) for 2 hours in male rats (Sprague-Dawley, 250–280 g) under anesthesia (20% chloral hydrate, body temperature 37°C). After recovery for different periods, the animals were killed and brains were rapidly removed, coronally sectioned at 2 mm, and stained with 2% 2,3,5-triphenyltetrazolium chloride (TTC, in 0.9% saline) for 15 minutes at 37°C. Infarct size was determined by digital planimetry of the slices using the Image-Pro software (Media Cybernetics Inc.) and normalized for edema. The infarct volume for each brain was calculated as *I*% = (volume of contralateral – normal volume of ipsilateral)/volume of contralateral. We measured regional cerebral blood flow (rCBF) by Laser-Doppler flowmetry (Moor Instruments Ltd.) with a probe fixed on the skull throughout the ischemia until 10 minutes after reperfusion (56). Rat intracerebroventricular injection was performed under anesthesia in a stereotaxic instrument (Stoelting Co.) using a microsyringe pump (Stoelting Co.). A scalp incision was made and 1 burr hole was opened in the right parietal skull, 1.7 mm lateral and 0.9 mm posterior to the bregma. A syringe was inserted into the brain to a depth of 3.8 mm below the cortical surface. The TAT-C6 (GRKKRRQRRRCRRGGSLKAAPGAGTRR) and TAT-ctrl (control1; GRKKRRQRRRCPPYGYYPSFRGNENRL or control2; GRKKRRQRRRC) peptides (5 mM/5 μl) were freshly dissolved in distilled water and were injected slowly (0.5 μl/min) into the right ventricle. The needle was kept in place for 10 minutes to allow diffusing into the ventricle. Distilled water (5 μl) was used as a vehicle control.

*Immunoblotting*. Samples for immunoblotting were prepared as described previously (57). The tissue samples were homogenized in 1:10 (w/v) ice-cold homogenized buffer containing: 10 mM Tris-Cl, pH 7.4, 150 mM NaCl, 5 mM EDTA, 1% Triton-X 100, 1 mM Na orthovanadate, 50 mM NaF, 5 mM DTT, and protease inhibitor cocktail (Sigma-Aldrich). The homogenates were centrifuged at 15,700 *g* for 15 minutes at 4°C. Supernatants were collected and protein concentrations were determined by the modified Lowry assay with bovine serum albumin as a standard. Samples were stored at –80°C until assay and were thawed only once. Cerebral cortical extracts (100 μg) were electrophoresed on SDS/7% PAGE and transferred to polyvinyldifluoridine membranes. The membranes were incubated overnight at 4°C with the primary antibodies followed by the horseradish peroxidase–conjugated anti-rabbit or anti-mouse secondary antibodies (Amersham Biosciences). The protein bands were visualized using the Amersham ECL system and scanned. The density of the bands was determined by ImageQuant (Amersham Biosciences).

*Reverse transcription and real-time PCR*. Total RNA was isolated by using TRIzol (Invitrogen) according to the manufacturer's protocol, and 5 μg of RNA was reverse transcribed with RevertAid M-MulV Reverse Transcriptase (MBI Fermentas) and 250 ng random primers (Invitrogen). Quantitative RT-PCR was performed as previously described (58). The following primer pairs were used for real-time PCR: GAPDH forward, 5′-ATGGGGAAGGTGAAGGTCG-3′; GAPDH reverse, 5′-GGGGTCATTGATGGCAACAATA-3′; TRPC 6 forward, 5′-GTCGGTGGTCATCAACTACAATC-3′; and TRPC 6 reverse, 5′-CCACATCCGCATCATCCTCAATT-3′ (59).

Quantification was done using the comparative $C_t$ method ($\Delta\Delta C_t$ method) as suggested by the manufacturer (Applied Biosystems). The cycle number at which the reaction crossed a threshold ($C_t$) was determined for the endogenous control (GAPDH) and target (TRPC6). The relative amount of TRPC6, normalized to the endogenous control and relative to a common reference sample was calculated by the formula $2^{-\Delta\Delta Ct}$. The reaction for the GAPDH and TRPC6 was carried out in triplicate for each sample.

*Immunohistochemistry and TUNEL staining*. The animals were perfused with 0.9% saline and then 4% paraformaldehyde in PBS (pH 7.4), and the brains was rapidly removed, then embedded in OCT solution (Sakura). Coronal or sagittal cryosections (14–20 μm) were made and examined by immunohistochemistry and TUNEL staining. Immunohistochemistry was performed on 14-μm–thick sections using rabbit polyclonal anti-TRPC6 (1:100; Millipore), mouse monoclonal anti-NeuN (1:200; Millipore), and mouse monoclonal anti-glial fibrillary acidic protein (1:200; Sigma-Aldrich). The Alexa Fluor 488 goat anti-rabbit IgG and Texas Red-X goat anti-mouse IgG (1:5000; Invitrogen) were secondary antibodies. Fluorescent signals were detected with a Nikon E800 epifluorescence microscope at excitation/emission wavelengths of 488/543 nm. The images were taken with a MicroFire digital color camera. For TRPC6 and TUNEL costaining, the slices were incubated with TRPC6 antibody and the in situ cell death detection kit (Roche) was then used to label the apoptotic cells according to the manufacturer's instructions.

*Cell culture, transfection, and OGD*. Rat primary cortical cultures (from 17-day-old embryonic SD rats) were prepared as described (60). The neurons were transfected using the Nucleofector Kit (Amaxa Biosystems) according to the manufacturer's instructions. For OGD, the culture medium was replaced by glucose-free Earle's balanced salt solution purged by nitrogen gas (5% $CO_2$ and 95% $N_2$) for 10 minutes. The cells were then placed for 2 hours in an anaerobic chamber (Forma Scientific) filled with 5% $CO_2$ and 95% $N_2$. The OGD was terminated by switching back to normal culture conditions. Cell death was assessed by propidium iodide (PI) staining. The TAT-C6 and TAT-ctrl peptides were freshly dissolved to 5 μM in the culture medium. After incubation for 20 minutes, the peptides were washed out and neuron cultures were subjected to OGD.

*Electrophysiology*. Recordings were performed on cortical neurons (DIV 10–12) in the whole cell configuration of the patch clamp technique, using a computer-controlled 700A amplifier (Axopatch 700A; Molecular Devices). To avoid contamination of $K^+$ current, pipettes (2–4 M) were filled with Cs pipette solution containing 140 mM CsCl, 0.3 mM $CaCl_2$, 10 mM EGTA, 1 mM $MgCl_2$, and 10 mM HEPES, pH 7.2. Normal extracellular solution contained 140 mM NaCl, 5 mM KCl, 1 mM $MgCl_2$, 1 mM $CaCl_2$, 10 mM D-glucose, and 10 mM HEPES, pH 7.4. To prevent voltage-dependent $Na^+$ current, 1 μM TTX was applied. CNQX (20 μM) was also used to limit synaptic activities. Holding potential was set at –60 mv. Recordings were filtered at 2 kHZ.

*$Ca^{2+}$ imaging*. The $[Ca^{2+}]_i$ measurement was performed as described previously (61). Briefly, cortical neurons were loaded with 2 μM Fura-2 AM (dissolved in 0.0125% Pluronic acid and diluted with DMSO) in HEPES-buffered saline (HPSS: 120 mM NaCl, 5.3 mM KCl, 0.8 mM $MgSO_4$, 1.8 mM $CaCl_2$, 11.1 mM glucose, and 20 mM HEPES, pH 7.4) for 30 minutes at 37°C, then washed with HPSS twice and incubated for another 30 minutes at 37°C. The $[Ca^{2+}]_i$ levels (F340/F380 ratio) were examined under a Nikon eclipse Te2000-e microscope with dual excitations of Fura-2 AM at 340 and 380 nm and detection of fluorescent emissions at 500 nm. Fluorescent images were collected every 3 seconds using a ×40 fluores-

cence oil objective for ratiometric $Ca^{2+}$ measurements. The $[Ca^{2+}]_i$ levels determined by the ratio F340/F380 were depicted as ΔR/R by MetaMorph software. All reagents were diluted to their final concentrations in HPSS and applied to the cells by surface perfusion. The duration of exposure to each reagent mixture is indicated by the horizontal lines under the traces depicting the changes in $[Ca^{2+}]_i$ as a function of time.

*In vitro calpain assay*. Adult rat brain lysates extracted with HEPES buffer (5 mM KCl, 1.5 mM $MgCl_2$, 1 mM dithiothreitol, 1 mM EGTA, and 20 mM HEPES, pH 7.4) were incubated with 1 mM $CaCl_2$ for 5–30 minutes at 37°C. Alternatively, the lysates (100 μl) were incubated with purified μ-calpain (BioVision) in the presence of 1 mM $CaCl_2$ for 30 minutes. For determination of the cleavage of TRPC6, HEK293 cells were transfected with *flag*-loop-*HA*-TRPC6-*myc* constructs by Lipofectamine 2000 (Invitrogen). The cell lysates were collected 24 hours later in the HEPES buffer and incubated with μ-calpain. The NUS-$C6_{1\text{-}203}$ purified by Ni-column (QIAGEN) was digested by calpain and the fragment with the N terminus of the cleavage was separated and transferred to the PVDF with CAPS buffer (10% methanol and 10 mM CAPS, pH 11). The band of 22 kDa was cut, and the Edman degradation analysis was conducted by Research Centre for Proteome Analysis (Shanghai, China).

*The rotarod assay*. The rat motor function analysis was performed by the rotarod test as previously reported (62). Briefly, rats were placed on the rotarod (Ugo Basile; Panlab Apparatus) set. The rotarod was accelerated uniformly from 4 to 40 rpm over 5 minutes. The animal latency to fall was recorded. The rats were trained 3 times per day for 3 days and on the morning of the experimental day in order to reduce the variability between subjects. Both training and test sessions were identical for TAT-ctrl– and TAT-C6–injected rats. We examined the motor function before surgery and 1, 7, 14, 21, and 35 days after ischemia/reperfusion.

*Antibodies and reagents*. We purchased antibodies from Alomone Labs (rabbit anti-TRPC1, -3, -4, -5, and -6 antibodies), Millipore (rabbit anti-TRPC6, mouse anti-NeuN, anti-GFAP, anti-spectrin, and anti-NR2A antibodies), Upstate Biotechnology Inc. (rabbit anti-GluR1, CREB, and phospho-CREB Ser133, and mouse anti-myc antibodies), Sigma-Aldrich (mouse anti–α-tubulin, rabbit anti-NR1, and anti-TRPC6 antibodies), and Santa Cruz Biotechnology Inc. ( goat anti-calpain 1 antibodies). Unless stated, all chemicals were from Sigma-Aldrich. The pCAGGS-IRES-GFP directs target gene expression by the CAGGS promoter and EGFP expression through IRES. The TRPC6 or DN-TRPC6 was subcloned into the pCAGGS-IRES-GFP vector. The TRPC6 was also subcloned into the pcDNA3 vector with *flag* (N terminus) and *myc* (C terminus) tag. The hemagglutinin (*HA*) epitope sequence (YPYDVPDYA) was inserted in tandem after $Gly^{572}$ of the TRPC6 primary sequence to place the epitope in the extracellular S3–S4 loop. The sequence that encoded the first 203 amino acids of TRPC6 was subcloned into the pET-43.1a vector (Novagen) to express an NUS-$C6_{1\text{-}203}$ fusion protein in *E. coli*.

*Statistics*. All data were presented as mean ± SEM. Statistical analysis was performed by either paired or unpaired 2-tailed Student's *t* tests. Statistically significant differences were defined as $P < 0.05$. The probability of survival was calculated using the nonparametric Kaplan-Meier method.

## Acknowledgments

We thank J.W. Putney Jr., T. Gudermann, D.J. Linden, and M.E. Greenberg for constructs; and Q. Hu and Z.J. Fan for technical assistance. This work was supported by grants from 973 Program (2006CB806600 and 2011CB809005), KSCX2-YW-R-099, and project 30711120566 from the National Natural Science Foundation (NNSF) of China.

Received for publication March 30, 2010, and accepted in revised form July 14, 2010.

Address correspondence to: Yizheng Wang, Institute of Neuroscience, Shanghai Institutes for Biological Sciences, Chinese Academy of Sciences, 320 Yue-Yang Road, Shanghai 200031, China. Phone: 86.21.5492.1793; Fax: 86.21.5492.1735; E-mail: yzwang@ion.ac.cn.

1. Dirnagl U, Iadecola C, Moskowitz MA. Pathobiology of ischaemic stroke: an integrated view. *Trends Neurosci*. 1999;22(9):391–397.
2. Lo EH, Dalkara T, Moskowitz MA. Mechanisms, challenges and opportunities in stroke. *Nat Rev Neurosci*. 2003;4(5):399–415.
3. Lipton P. Ischemic cell death in brain neurons. *Physiol Rev*. 1999;79(4):1431–1568.
4. Choi DW. Ischemia-induced neuronal apoptosis. *Curr Opin Neurobiol*. 1996;6(5):667–672.
5. Hoyte L, Barber PA, Buchan AM, Hill MD. The rise and fall of NMDA antagonists for ischemic stroke. *Curr Mol Med*. 2004;4(2):131–136.
6. Prass K, Dirnagl U. Glutamate antagonists in therapy of stroke. *Restor Neurol Neurosci*. 1998; 13(1–2):3–10.
7. Ginsberg MD. Neuroprotection for ischemic stroke: past, present and future. *Neuropharmacology*. 2008;55(3):363–389.
8. Wes PD, Chevesich J, Jeromin A, Rosenberg C, Stetten G, Montell C. TRPC1, a human homolog of a Drosophila store-operated channel. *Proc Natl Acad Sci U S A*. 1995;92(21):9652–9656.
9. Zhu X, Chu PB, Peyton M, Birnbaumer L. Molecular cloning of a widely expressed human homologue for the Drosophila trp gene. *FEBS Lett*. 1995;373(3):193–198.
10. Montell C, Birnbaumer L, Flockerzi V. The TRP channels, a remarkably functional family. *Cell*. 2002;108(5):595–598.
11. Harteneck C, Plant TD, Schultz G. From worm to man: three subfamilies of TRP channels. *Trends Neurosci*. 2000;23(4):159–166.
12. Clapham DE. TRP channels as cellular sensors. *Nature*. 2003;426(6966):517–524.
13. Vazquez G, Wedel BJ, Aziz O, Trebak M, Putney JW Jr. The mammalian TRPC cation channels. *Biochim Biophys Acta*. 2004;1742(1–3):21–36.
14. Li Y, et al. Essential role of TRPC channels in the guidance of nerve growth cones by brain-derived neurotrophic factor. *Nature*. 2005;434(7035):894–898.
15. Greka A, Navarro B, Oancea E, Duggan A, Clapham DE. TRPC5 is a regulator of hippocampal neurite length and growth cone morphology. *Nat Neurosci*. 2003;6(8):837–845.
16. Yu Y, et al. Enhanced expression of transient receptor potential channels in idiopathic pulmonary arterial hypertension. *Proc Natl Acad Sci U S A*. 2004;101(38):13861–13866.
17. Riccio A, et al. Essential role for TRPC5 in amygdala function and fear-related behavior. *Cell*. 2009;137(4):761–772.
18. Jia Y, Zhou J, Tai Y, Wang Y. TRPC channels promote cerebellar granule neuron survival. *Nat Neurosci*. 2007;10(5):559–567.
19. Justicia C, Planas AM. Transforming growth factor-alpha acting at the epidermal growth factor receptor reduces infarct volume after permanent middle cerebral artery occlusion in rats. *J Cereb Blood Flow Metab*. 1999;19(2):128–132.
20. Vennekens R, Voets T, Bindels RJ, Droogmans G, Nilius B. Current understanding of mammalian TRP homologues. *Cell Calcium*. 2002;31(6):253–264.
21. Nilius B, Voets T. Diversity of TRP channel activation. *Novartis Found Symp*. 2004;258:140–149.
22. Saarelainen T, et al. Transgenic mice overexpressing truncated trkB neurotrophin receptors in neurons show increased susceptibility to cortical injury after focal cerebral ischemia. *Mol Cell Neurosci*. 2000;16(2):87–96.
23. Longa EZ, Weinstein PR, Carlson S, Cummins R. Reversible middle cerebral artery occlusion without craniectomy in rats. *Stroke*. 1989;20(1):84–91.
24. Goldberg MP, Choi DW. Combined oxygen and glucose deprivation in cortical cell culture: calcium-dependent and calcium-independent mechanisms of neuronal injury. *J Neurosci*. 1993;13(8):3510–3524.
25. Hofmann T, Obukhov AG, Schaefer M, Harteneck C, Gudermann T, Schultz G. Direct activation of human TRPC6 and TRPC3 channels by diacylglycerol. *Nature*. 1999;397(6716):259–263.
26. Inoue R, et al. The transient receptor potential protein homologue TRP6 is the essential component of vascular alpha(1)-adrenoceptor-activated Ca(2+)-permeable cation channel. *Circ Res*. 2001; 88(3):325–332.
27. Merritt JE, et al. SK&F 96365, a novel inhibitor of receptor-mediated calcium entry. *Biochem J*. 1990;271(2):515–522.
28. Hofmann T, Schaefer M, Schultz G, Gudermann T. Subunit composition of mammalian transient receptor potential channels in living cells. *Proc Natl Acad Sci U S A*. 2002;99(11):7461–7466.
29. Xiong ZG, et al. Neuroprotection in ischemia: blocking calcium-permeable acid-sensing ion channels. *Cell*. 2004;118(6):687–698.
30. Mabuchi T, et al. Phosphorylation of cAMP response element-binding protein in hippocampal neurons as a protective response after exposure to glutamate in vitro and ischemia in vivo. *J Neurosci*. 2001;21(23):9204–9213.
31. Walton M, Sirimanne E, Williams C, Gluckman P,

Dragunow M. The role of the cyclic AMP-responsive element binding protein (CREB) in hypoxic-ischemic brain damage and repair. *Brain Res Mol Brain Res*. 1996;43(1–2):21–29.
32. Siman R, Baudry M, Lynch G. Brain fodrin: substrate for calpain I, an endogenous calcium-activated protease. *Proc Natl Acad Sci U S A*. 1984;81(11):3572–3576.
33. Siman R, Noszek JC. Excitatory amino acids activate calpain I and induce structural protein breakdown in vivo. *Neuron*. 1988;1(4):279–287.
34. del Cerro S, et al. Stimulation of NMDA receptors activates calpain in cultured hippocampal slices. *Neurosci Lett*. 1994;167(1–2):149–152.
35. Siman R, Bozyczko-Coyne D, Savage MJ, Roberts-Lewis JM. The calcium-activated protease calpain I and ischemia–induced neurodegeneration. *Adv Neurol*. 1996;71:167–174.
36. Hamakubo T, Kannagi R, Murachi T, Matus A. Distribution of calpains I and II in rat brain. *J Neurosci*. 1986;6(11):3103–3111.
37. Vives E, Brodin P, Lebleu B. A truncated HIV-1 Tat protein basic domain rapidly translocates through the plasma membrane and accumulates in the cell nucleus. *J Biol Chem*. 1997;272(25):16010–16017.
38. Mattson MP. Neuroprotective signal transduction: relevance to stroke. *Neurosci Biobehav Rev*. 1997; 21(2):193–206.
39. Walton MR, Dragunow I. Is CREB a key to neuronal survival? *Trends Neurosci*. 2000;23(2):48–53.
40. Finkbeiner S. CREB couples neurotrophin signals to survival messages. *Neuron*. 2000;25(1):11–14.
41. Kitagawa K. CREB and cAMP response element-mediated gene expression in the ischemic brain. *FEBS J*. 2007;274(13):3210–3217.
42. Hunter AJ, Mackay KB, Rogers DC. To what extent have functional studies of ischaemia in animals been useful in the assessment of potential neuroprotective agents? *Trends Pharmacol Sci*. 1998;19(2):59–66.
43. Aarts M, et al. A key role for TRPM7 channels in anoxic neuronal death. *Cell*. 2003;115(7):863–877.
44. Sun HS, et al. Suppression of hippocampal TRPM7 protein prevents delayed neuronal death in brain ischemia. *Nat Neurosci*. 2009;12(10):1300–1307.
45. Sugawara T, Chan PH. Reactive oxygen radicals and pathogenesis of neuronal death after cerebral ischemia. *Antioxid Redox Signal*. 2003;5(5):597–607.
46. Halliwell B. Free radicals, antioxidants, and human disease: curiosity, cause, or consequence? *Lancet*. 1994;344(8924):721–724.
47. Lindsay RM. Role of neurotrophins and trk receptors in the development and maintenance of sensory neurons: an overview. *Philos Trans R Soc Lond B Biol Sci*. 1996;351(1338):365–373.
48. Lykissas MG, Batistatou AK, Charalabopoulos KA, Beris AE. The role of neurotrophins in axonal growth, guidance, and regeneration. *Curr Neurovasc Res*. 2007;4(2):143–151.
49. Venkatachalam K, Montell C. TRP channels. *Annu Rev Biochem*. 2007;76:387–417.
50. Dietrich A, et al. Increased vascular smooth muscle contractility in TRPC6$^{-/-}$ mice. *Mol Cell Biol*. 2005;25(16):6980–6989.
51. Trebak M, Vazquez G, Bird GS, Putney JW Jr. The TRPC3/6/7 subfamily of cation channels. *Cell Calcium*. 2003;33(5–6):451–461.
52. Dietrich A, Mederos y Schnitzler M, Emmel J, Kalwa H, Hofmann T, Gudermann T. N-linked protein glycosylation is a major determinant for basal TRPC3 and TRPC6 channel activity. *J Biol Chem*. 2003;278(48):47842–47852.
53. Kubbutat MH, Vousden KH. Proteolytic cleavage of human p53 by calpain: a potential regulator of protein stability. *Mol Cell Biol*. 1997;17(1):460–468.
54. Huang C, Rajfur Z, Yousefi N, Chen Z, Jacobson K, Ginsberg MH. Talin phosphorylation by Cdk5 regulates Smurf1-mediated talin head ubiquitylation and cell migration. *Nat Cell Biol*. 2009;11(5):624–630.
55. Lee MS, Kwon YT, Li M, Peng J, Friedlander RM, Tsai LH. Neurotoxicity induces cleavage of p35 to p25 by calpain. *Nature*. 2000;405(6784):360–364.
56. Herrmann O, et al. IKK mediates ischemia-induced neuronal death. *Nat Med*. 2005;11(12):1322–1329.
57. Ashwal S Tone B, Tian HR Cole DJ, Pearce WJ. Core and penumbral nitric oxide synthase activity during cerebral ischemia and reperfusion. *Stroke*. 1998;29(5):1037–1046.
58. Wang ZH, et al. Blockage of intermediate-conductance-Ca(2+) -activated K(+) channels inhibits progression of human endometrial cancer. *Oncogene*. 2007;26(35):5107–5114.
59. Tai K, Hamaide MC, Debaix H, Gailly P, Wibo M, Morel N. Agonist-evoked calcium entry in vascular smooth muscle cells requires IP3 receptor-mediated activation of TRPC1. *Eur J Pharmacol*. 2008;583(1):135–147.
60. Tao Y, Yan D, Yang Q, Zeng R, Wang Y. Low K+ promotes NF-kappaB/DNA binding in neuronal apoptosis induced by K+ loss. *Mol Cell Biol*. 2006;26(3):1038–1050.
61. Zhu X, et al. trp, a novel mammalian gene family essential for agonist-activated capacitative Ca2+ entry. *Cell*. 1996;85(5):661–671.
62. Hamm RJ, Pike BR, O'Dell DM, Lyeth BG, Jenkins LW. The rotarod test: an evaluation of its effectiveness in assessing motor deficits following traumatic brain injury. *J Neurotrauma*. 1994;11(2):187–196.